ASME Journal of Biomechanical Engineering
Online journal at:
https://asmedigitalcollection.asme.org/biomechanical

Influence of Walking Over Unexpected Uneven Terrain on Joint Loading for Individuals With Transtibial Amputation

Kristen M. Stewart
Walker Department of Mechanical Engineering,
The University of Texas at Austin,
204 East Dean Keeton Street,
Austin, TX 78712-1591
e-mail: kristen.stewart@utexas.edu

Glenn K. Klute
Department of Veterans Affairs,
Puget Sound Health Care System,
1660 South Columbian Way, MS-151,
Seattle, WA 98118;
Department of Mechanical Engineering,
University of Washington,
3900 East Stevens Way NE,
Seattle, WA 98195
e-mail: gklute@uw.edu

Richard R. Neptune[1]
Walker Department of Mechanical Engineering,
The University of Texas at Austin,
204 East Dean Keeton Street,
Austin, TX 78712-1591
e-mail: rneptune@mail.utexas.edu

Individuals with transtibial amputation (TTA) experience asymmetric lower-limb loading which can lead to joint pain and injuries. However, it is unclear how walking over unexpected uneven terrain affects their loading patterns. This study sought to use modeling and simulation to determine how peak joint contact forces and impulses change for individuals with unilateral TTA during an uneven step and subsequent recovery step and how those patterns compare to able-bodied individuals. We expected residual limb loading during the uneven step and intact limb loading during the recovery step would increase relative to flush walking. Further, individuals with TTA would experience larger loading increases compared to able-bodied individuals. Simulations of individuals with TTA showed during the uneven step, changes in joint loading occurred at all joints except the prosthetic ankle relative to flush walking. During the recovery step, intact limb joint loading increased in early stance relative to flush walking. Simulations of able-bodied individuals showed large increases in ankle joint loading for both surface conditions. Overall, increases in early stance knee joint loading were larger for those with TTA compared to able-bodied individuals during both steps. These results suggest that individuals with TTA experience altered joint loading patterns when stepping on uneven terrain. Future work should investigate whether an adapting ankle-foot prosthesis can mitigate these changes to reduce injury risk. [DOI: 10.1115/1.4065045]

Keywords: musculoskeletal model, simulation, below-knee, biomechanics

1 Introduction

Individuals with transtibial amputation (TTA) are faced with challenges during activities of daily living, particularly when encountering unanticipated uneven terrain commonly found outdoors. In middle-aged and older adults, more than 70% of falls occur due to environmental factors [1]. Individuals with TTA are at an even higher risk of falling compared to able-bodied (AB) individuals and are more likely to sustain life-altering injuries [2].

In response to surface perturbations, AB individuals can quickly invoke several response mechanisms to restore their balance, such as conforming their foot to the surface and producing an inversion or eversion moment to prevent further ankle rotation [3]. AB individuals can also use a lateral ankle strategy to shift the center of pressure or a hip strategy to alter the ground reaction forces (GRFs) [4–7].

In contrast, individuals with TTA are unable to use similar ankle response strategies due to the limited degrees-of-freedom of commonly prescribed prostheses and the lack of ankle muscles in the residual limb. As a result, individuals with TTA often have an increased reliance on the hip strategy to recover from foot-placement perturbations [8] or an increased reliance on the recovery step following an unexpected step on uneven terrain [9]. Further, these individuals have a higher range of whole-body angular momentum [10,11], which is a common measure to assess balance control [12]. A higher range of angular momentum and increased center-of-mass movement compared to healthy individuals [13] suggests individuals with TTA have poorer balance control and a greater fall risk. These individuals also often adopt a more conservative gait with shorter and wider steps with a greater variability in foot placement across uneven surfaces compared to level-ground walking [14].

During level-ground walking, individuals with TTA often display asymmetric gait patterns, leading to asymmetric joint moments at the hip and knee [15] and higher knee adduction moments, medial knee contact forces, and loading rate in the intact limb compared to the residual limb [16]. In addition, peak axial knee joint contact loading in the intact limb is higher in early stance compared to the residual limb or AB individuals during flush walking [17]. These characteristics are thought to contribute to the development of joint pain and injuries [18,19], as individuals with TTA often develop osteoarthritis in the intact limb knee [20–22] or hip [22,23]. These deviations in lower-limb joint loading may be further exacerbated when an individual with TTA encounters an uneven surface. Previous work has shown the direction of the uneven surface (e.g., inversion versus eversion) elicits a different response [13], which may further affect joint loading for individuals with TTA.

Joint contact forces (JCF) are difficult to measure experimentally without surgical intervention such as using instrumented implants [24–27]. Often, joint moments are used as a surrogate measure to

[1]Corresponding author.
Manuscript received August 30, 2023; final manuscript received February 22, 2024; published online April 8, 2024. Assoc. Editor: Bruce MacWilliams.

describe joint contact loading using an inverse-dynamics approach [28–30]. While the knee adduction moment has been correlated to the presence of knee osteoarthritis [19,31], the correlation between knee moment and JCF has not been consistent throughout the gait cycle [32,33]. The inverse dynamics approach only accounts for the inertial and GRF contributions to joint loading and does not account for muscle forces crossing each joint, which have been shown to be significant contributors to JCF [34,35]. Therefore, musculoskeletal modeling and simulation, which can be used to estimate JCF, is a promising approach to assessing the influence of stepping on an uneven surface on joint loading for those with TTA.

The purpose of this study was to determine how lower-limb joint loading is affected while stepping on a coronally uneven surface and during the subsequent recovery step in individuals with unilateral TTA and AB individuals using musculoskeletal modeling and simulation. We expected that residual limb loading during the uneven step and intact limb loading during the recovery step would increase relative to flush walking. We also expected that the relative difference in joint loading between conditions would be greater for individuals with TTA compared to AB individuals.

2 Methods

2.1 Experimental Data. Experimental data were previously collected at the Department of Veterans Affairs Center for Limb Loss and Mobility. Five individuals with unilateral TTA (3 male; age: 49.4 ± 14.4 years; height: 1.71 ± 0.10 m; weight: 79.0 ± 14.2 kg; self-selected walking speed: 1.30 ± 0.15 m/s) wearing their clinically prescribed prosthesis and five AB individuals (3 male; age: 52.8 ± 16.1 years; height: 1.69 ± 0.07 m; weight: 69.8 ± 12.7 kg; self-selected walking speed: 1.33 ± 0.10 m/s) [36] were among the sample population who provided their informed consent and completed all procedures in this Institutional Review Board approved protocol. All participants were able to ambulate without upper extremity aids. Individuals with TTA had all been fitted with a prosthesis and used it for at least six months for at least four hours per day by self-report. The specific components of each individual with TTA's prosthesis were not controlled, rather each wore the prosthesis that they and their clinician had previously agreed was best suited to meet their daily ambulatory needs.

All subjects walked at their self-selected speed over ground on a walkway embedded with five force plates (AMTI, Watertown, MA), with the center plate of the walkway (Kistler, Winterthur, Switzerland) oriented either flush or rotated coronally ±15 deg to cause ankle inversion or eversion. The rotation of the plate was manually positioned using a custom jig which was recessed into the walkway (see Ref. [9]). Individuals with TTA contacted the center plate with their residual limb and AB individuals with their dominant limb. The subjects completed steady-state trials where the plate rotation was visible for each condition. Then, the plate rotation was blinded to the participant by covering the plate with an elastic, opaque cover to minimize anticipatory compensations. Subjects were not instructed to target the center plate. Only trials with a single-foot contact on the center plate were included in the analysis. Five successful trials were performed for each condition and the order of the blinded conditions was randomized.

Kinematic data were collected using a 12-camera motion-capture system (Vicon Motion Systems Ltd, Oxford, GBR) at 120 Hz, and kinetic and electromyography (EMG) data were collected at 1200 Hz for each trial. Lower-limb EMG data were collected using bilateral electrodes placed on the gluteus maximus (GMAX), gluteus medius (GMED), biceps femoris long head (BFLH), rectus femoris (RF), vastus medialis (VAS) and tibialis anterior (TA) for all subjects with medial gastrocnemius (GAS) and peroneus longus (PL) for AB individuals. Kinematic and kinetic data were filtered with a fourth-order low-pass Butterworth filter with cutoff frequencies of 6 Hz and 15 Hz, respectively. EMG data were high-pass filtered at 40 Hz, demeaned, rectified, low-pass filtered at 4 Hz, and normalized to the peak activation per trial.

2.2 Modeling and Simulation. For each subject, trials were selected based on representative kinematics and kinetics using a functional median depth method [37]. A previously developed three-dimensional musculoskeletal model with 23 degrees-of-freedom and 92 Hill-type musculotendon actuators was used in OpenSim 4.2 [38] for AB individuals. The model was modified for individuals with TTA by adjusting the tibia segment, including a rigid pylon socket and ankle-foot prosthesis with previously described inertial properties [39], and removing the muscles spanning the ankle for 79 total musculotendon actuators. The ankle-foot prosthesis was modeled as a one degree-of-freedom pin joint with a coordinate actuator to account for the motion at the ankle. Each model was scaled to match the anthropometrics of each subject.

Simulations were performed for each individual with TTA and AB individual in steady-state flush and blinded eversion and inversion conditions for a total of 30 simulations. Each simulation included the uneven step (with the residual limb for individuals with TTA or dominant foot for AB individuals) and the subsequent recovery step (with the intact limb for individuals with TTA or nondominant foot for AB individuals). Inverse kinematics estimated the body segment kinematics from marker data in each trial, and a residual reduction algorithm [38] then adjusted the model segments' mass and the torso center-of-mass to minimize dynamic discrepancies between kinematic and kinetic data. A forward dynamics approach utilizing a computed muscle control (CMC) algorithm [40] solved for muscle excitations at each time point that tracked the desired kinematics and minimized the sum of activations squared to reduce un-necessary coactivation. The muscle activation results from the simulation were compared to available EMG data to assure the muscles were generating force at the appropriate phases of the gait cycle.

2.3 Joint Loading. Joint reaction force analyses were performed in OpenSim to determine the JCF, which accounts for the forces from passive structures, muscle forces, and the corresponding motion. The JCF was calculated at both hip and knee joints for all subjects, both ankle joints for AB individuals, and the intact and prosthetic ankle joint for individuals with TTA. The JCF was normalized by each subject's body mass and separated for analysis into the uneven step and recovery step stance phases. Joint contact impulses (JCIs) were computed by integrating the JCF over the stance time and separated into early (first half) and late (second half) stances. Peak JCFs and JCIs were computed for flush, inverted, and everted conditions and averaged within each subject group.

2.4 Statistical Analysis. Due to the small sample size, the comparisons across conditions were limited to confidence intervals and descriptive statistics. Linear mixed-effects models were used in MATLAB (Mathworks, Natick, MA) to calculate the 95% confidence intervals for each JCI surface condition. The fixed effects were the subject groups (AB individual or individual with TTA) and surface condition (flush, everted, or inverted), with a random effect of subject. Descriptive statistics were included for percent differences between uneven conditions and flush for both peak JCF and JCI. For comparison between conditions, any percent difference greater than 10% was considered substantial, as this threshold represents a change in joint loading measures above the minimal detectable change reported in Barrios and Willson [41].

3 Results

3.1 Simulation Results. Each scaled model had a maximum marker error of less than 2 cm and root-mean-square error of less than 1 cm. The kinematics tracked experimental data well, with average errors of 0.98 degrees for rotational values and 0.56 cm for translational values. Average residual forces and moments applied to the pelvis were 0.64 N and 0.55 Nm, respectively, for individuals with TTA, and 1.10 N and 0.32 Nm, respectively, for AB individuals for all simulations. Additional average reserve moments at each

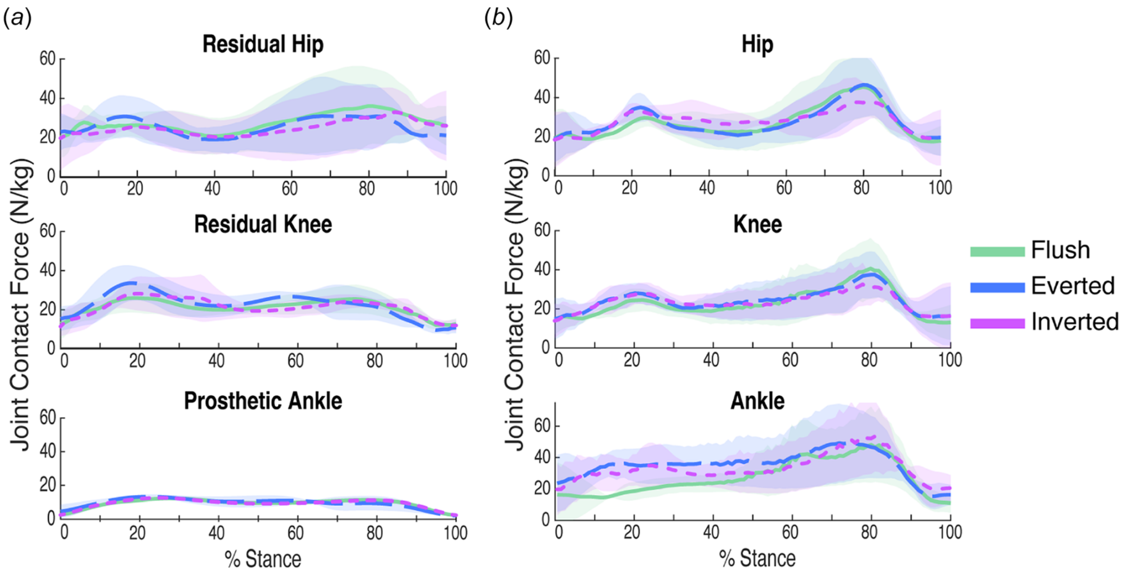

Fig. 1 (*a*) Joint contact force at the hip, knee and prosthetic ankle for individuals with TTA and (*b*) hip, knee and ankle for AB individuals during the uneven step stance phase for flush, everted and inverted conditions. Each force was normalized by body mass and averaged across subjects.

joint to track the desired kinematics were less than 3.60 Nm for all subjects. Muscle activation profiles from the simulations were similar to normalized EMG data for most muscles, such as the residual and intact limb GMED and BFLH and intact limb TA and GAS. However, there were differences in magnitude of muscle activations for some muscles such as the residual and intact limb RF and the intact limb PL. The most notable differences between conditions were observed in the magnitude of the residual and intact limb GMED. Muscle activation profiles are provided in Appendix A (Figs. 5–7).

3.2 Uneven Step. During early stance of the uneven step, individuals with TTA demonstrated increased peak residual knee JCF for the everted surface (30%) compared to flush (Fig. 1(*a*)). There was an increase in peak hip JCF for the everted surface (11%). AB individuals also demonstrated increased peak knee JCF (Fig. 1(*b*)) for the everted (14%) and inverted (14%) surfaces. However, the relative increase in peak knee JCF in the everted surface was higher for individuals with TTA compared to AB individuals (30% versus 14%). AB individuals experienced the largest change in joint loading at the ankle, with increased JCF for both everted (35%) and inverted (24%) surfaces compared to flush (Fig. 1(*b*)).

Individuals with TTA experienced increased JCI in early stance at the residual knee (20% versus 12%) (Fig. 2(*a*)), whereas AB individuals experienced increased ankle JCI (58% versus 36%) (Fig. 2(*b*)) for everted and inverted surfaces, respectively, compared to flush. Individuals with TTA experienced a greater average increase in response to uneven surface conditions in knee JCI compared to AB individuals.

In late stance, there was a decrease in peak hip JCF for the everted surface (−14%) for individuals with TTA (Fig. 1(*a*)). No notable changes in prosthetic ankle JCF were present in response to surface condition. AB individuals displayed decreased peak JCF at the knee (−16%) and hip (−20%) for the inverted surface, with no changes for the everted surface compared to flush (Fig. 1(*b*)).

Average JCI decreased at the residual hip for individuals with TTA (everted: −13%; inverted: −11%) (Fig. 2(*c*)) and AB individuals (inverted: −14%), with a decrease in knee JCI (inverted: −16%) only for AB compared to flush (Fig. 2(*d*)). Individuals with TTA experienced a smaller average decrease in knee JCI and lower magnitudes of knee and ankle JCI compared to AB individuals. All relative changes during the uneven step for JCF are provided in Appendix B (Tables 1 and 2) and JCI are provided in Appendix B (Tables 3 and 4).

3.3 Recovery Step. During early stance of the recovery step for individuals with TTA, the everted and inverted surface conditions produced higher peak hip (24% and 14%) and knee JCF (11% and 16%), respectively, compared to flush (Fig. 3(*a*)). The increase in peak forces at all joints for AB individuals was similar for both uneven surfaces compared to flush (Fig. 3(*b*)). The relative changes in peak hip JCF and the magnitude of peak knee JCF were larger for both conditions in individuals with TTA relative to AB individuals.

Individuals with TTA experienced increases in early stance JCI at all intact joints (hip: 17% versus 15%; knee: 10% versus 8%; ankle: 22% versus 15%) for everted and inverted surfaces, respectively, relative to flush (Fig. 4(*a*)). AB individuals also experienced increases in knee (inverted: 15%) and ankle JCI (everted: 17%; inverted: 30%) and no notable change in hip JCI in either surface compared to flush (Fig. 4(*b*)). Individuals with TTA experienced larger increases in hip JCI for both surface conditions and knee JCI for the everted surface compared to AB individuals. In addition, the magnitude of knee JCI was larger for individuals with TTA compared to AB individuals.

In late stance, individuals with TTA had an increase in peak intact hip JCF for the inverted surface (13%) and a decrease for the everted surface (−19%) compared to flush (Fig. 3(*a*)). There were increases in peak intact knee (11% versus 16%) and ankle (15% versus 11%) JCF for both everted and inverted surfaces, respectively, relative to flush. AB individuals experienced no notable changes in peak JCF at all joints in response to the inverted surface and reduced peak JCF at all joints in response to the everted surface relative to flush (Fig. 3(*b*)). The relative changes in peak hip and knee JCF were larger for individuals with TTA compared to AB individuals.

Average JCI for individuals with TTA increased at all intact joints in the uneven surface conditions relative to flush, except for a slight decrease at the hip during the everted surface (Fig. 4(*c*)). AB individuals experienced decreased JCI at all joints during the everted and inverted surfaces relative to flush (Fig. 4(*d*)). All relative changes for recovery step JCF are provided in Appendix B (Tables 1 and 2) and JCI are provided in Appendix B (Tables 3 and 4).

4 Discussion

4.1 Uneven Step. The simulation results revealed there were increases in joint loading in specific regions of the gait cycle when individuals with TTA encountered uneven terrain. While some joints have higher JCF on uneven surfaces compared to flush (early stance residual hip and knee), the trends were not consistent across the gait cycle (late stance residual hip)

(Fig. 1(*a*)). These results suggest there were unequal compensations occurring throughout the gait cycle in response to the uneven surface.

Knee JCI increased for both surface conditions for individuals with TTA (Fig. 2(*a*)). There was only a change in the residual knee JCF trajectory for the everted step (Fig. 1(*a*)), but stance time increased for the everted (2.5%) and inverted (5%) surfaces compared to the flush condition. The stance time increase was consistent with previous work which showed that individuals with TTA walk on unfamiliar terrain at a reduced walking speed [42]. A more cautious gait is also consistent with increased mediolateral center-of-mass movement during a coronally uneven step [7] and poorer balance control for individuals with TTA than AB individuals [10,13,43].

Overall, individuals with TTA had larger relative changes in early stance residual knee JCF and JCI between conditions compared to AB individuals (Figs. 1 and 2). Consistent with other simulation results [17], there was a higher magnitude of JCI for AB individuals in late stance, but these individuals had a larger decrease between conditions. The lack of change in late stance residual knee JCI for individuals with TTA (Fig. 2(*c*)) may suggest an increased reliance on their intact limb during the recovery step. This finding is consistent with other studies that identified compensatory mechanisms on the intact limb through various kinematic and kinetic measures [9,17,44,45].

The limited degrees-of-freedom of currently-prescribed prosthetic ankle-feet may account for the observed differences in ankle joint loading between individuals with TTA and AB individuals. The peak prosthetic ankle loading did not change between conditions for individuals with TTA (Fig. 2(*a*)), whereas the largest changes in loading between conditions occurred at the ankle for AB individuals (Fig. 2(*b*)). The magnitude of prosthetic ankle JCI was also lower for individuals with TTA compared to AB individuals for all conditions. This suggests that individuals with TTA may rely on compensations at other joints, such as the intact limb hip and knee, where changes were not as notable for AB individuals. Previous work has shown that in addition to AB individuals having the ability to conform their foot to the surface, they also demonstrate differing forefoot-hindfoot and hindfoot-tibia loading, which suggests a need for prostheses to mimic ankle and foot adaptations [3]. The results of this study further support the idea that prostheses need to account for natural adaptations to uneven surfaces, which could allow for ankle joint loading resembling AB individuals, leading to a reduction in increases in joint loading across other joints while stepping on uneven surfaces. With improved development of adapting prostheses, clinicians should consider whether individuals with TTA often ambulate outdoor terrain during the prosthesis prescription process to help reduce the risk of overuse injuries, as reflected by increased JCI for individuals with TTA.

4.2 Recovery Step. During recovery stance, peak intact knee and hip JCF for individuals with TTA increased during early stance but were not consistent throughout late stance (Fig. 3(*a*)). These results further support that there were different compensations across joints when individuals with TTA encountered an uneven surface.

While the relative increase in peak JCF at the hip and knee were not all larger for individuals with TTA (Fig. 3(*a*)) compared to AB individuals (Fig. 3(*b*)), the magnitude of peak JCF was higher. Previous work has shown that the magnitude of the peak JCF is larger in the intact knee compared to AB individuals [17], consistent with our results in early recovery stance (Fig. 3(*a*)). Since joint loading has been suggested as a contributor to knee osteoarthritis [19], this increase in intact knee peak joint loading could further increase the injury risk for individuals with TTA.

The increase in intact hip and knee JCI in early stance for individuals with TTA (Fig. 4(*a*)) is consistent with the trends that peak intact hip and knee loading increased during uneven surface conditions relative to flush. In addition, relative increases in early stance intact hip JCI and early and late stance intact knee JCI between conditions for individuals with TTA (Figs. 4(*a*) and 4(*c*))

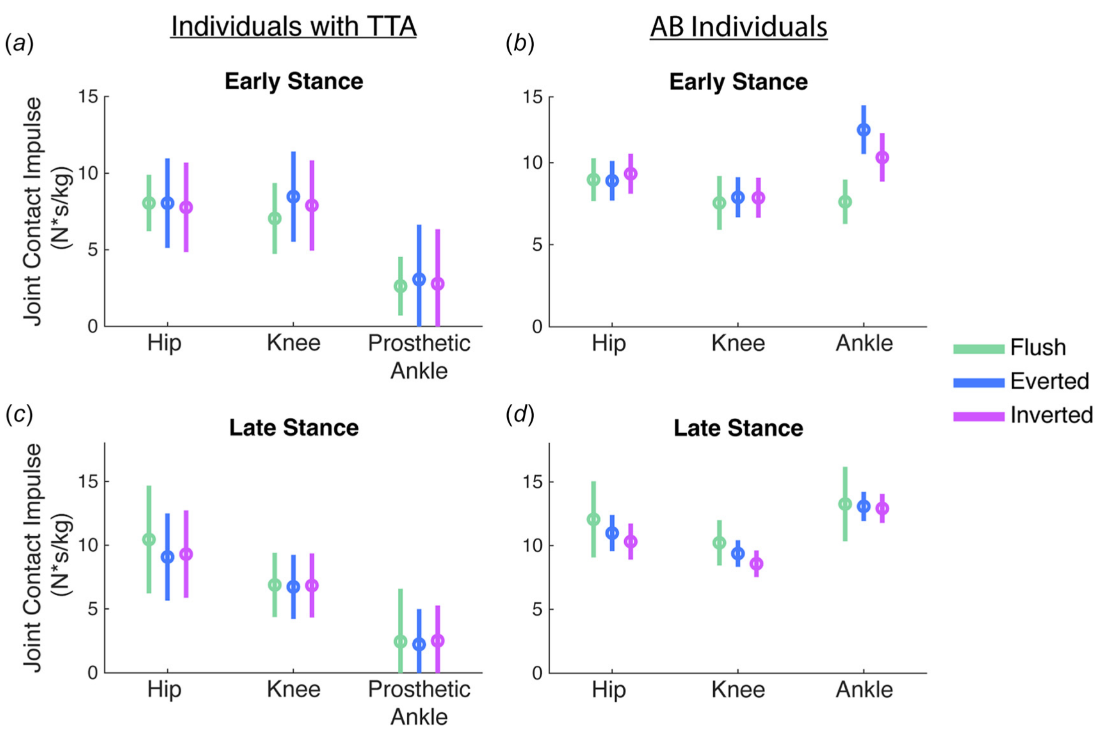

Fig. 2 **(*a*) Residual limb for individuals with TTA and (*b*) dominant limb for AB individuals joint contact impulse (JCI) during early stance in the flush, everted, and inverted uneven step conditions. (*c*) Residual limb for individuals with TTA and D) dominant limb for AB individuals JCI during late stance in the flush, everted, and inverted uneven step conditions. Early and late stance are determined by the first or second half of stance, respectively. All impulses are normalized by body mass. Open circles represent mean JCI and vertical bars represent 95% confidence intervals for each condition.**

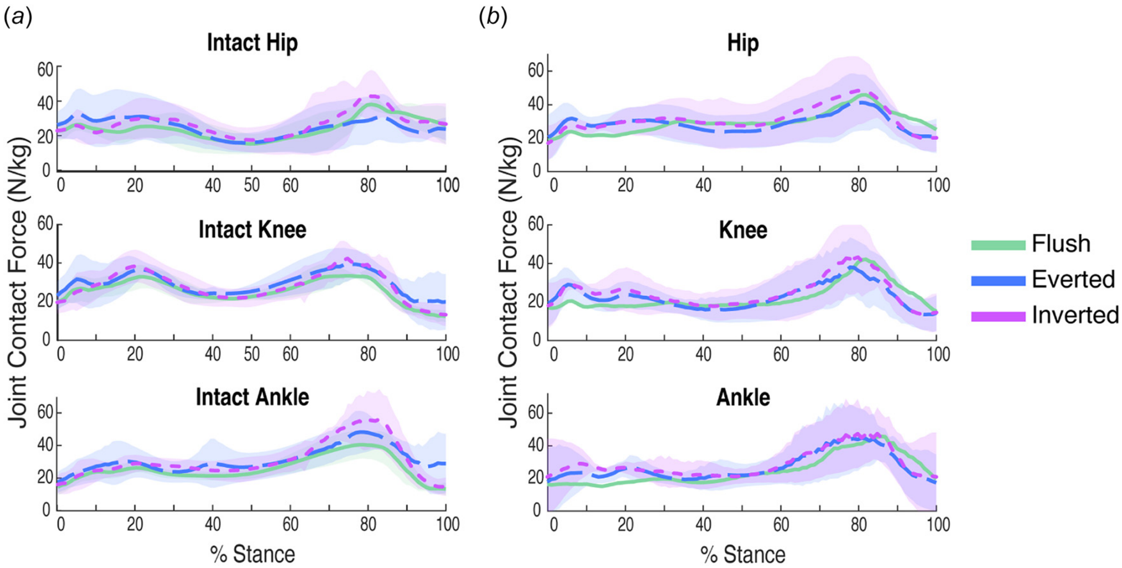

Fig. 3 **(*a*) Joint contact force at the hip, knee and ankle for individuals with TTA and (*b*) AB individuals during the recovery step stance phase for flush, everted, and inverted conditions. Each force was normalized by body mass and averaged across subjects.**

were larger than the increases for AB individuals (Figs. 4(*b*) and 4(*d*)). Thus, future studies should investigate how different compensatory strategies contribute to joint loading and if some strategies lead to lower joint loads.

4.3 Limitations. Differences in joint loading may have been caused in part by the experimental foot placement location on the uneven surface. The rotated step was lower than the flush surface so the subjects would be blinded to the condition. As a result, the mediolateral foot position affected the severity of the perturbation for individuals with TTA who could not fully conform their foot to the surface and caused slight differences in the vertical contact point. However, vertical center-of-mass position and vertical GRF impulse remained unchanged between conditions [9], suggesting the vertical change in foot position did not significantly impact the results.

In vivo measurements would provide more accurate measurements for determining joint contact loading but would not be feasible for measuring every individual at multiple joints. CMC has been shown to overestimate the muscle activations [46], and muscle

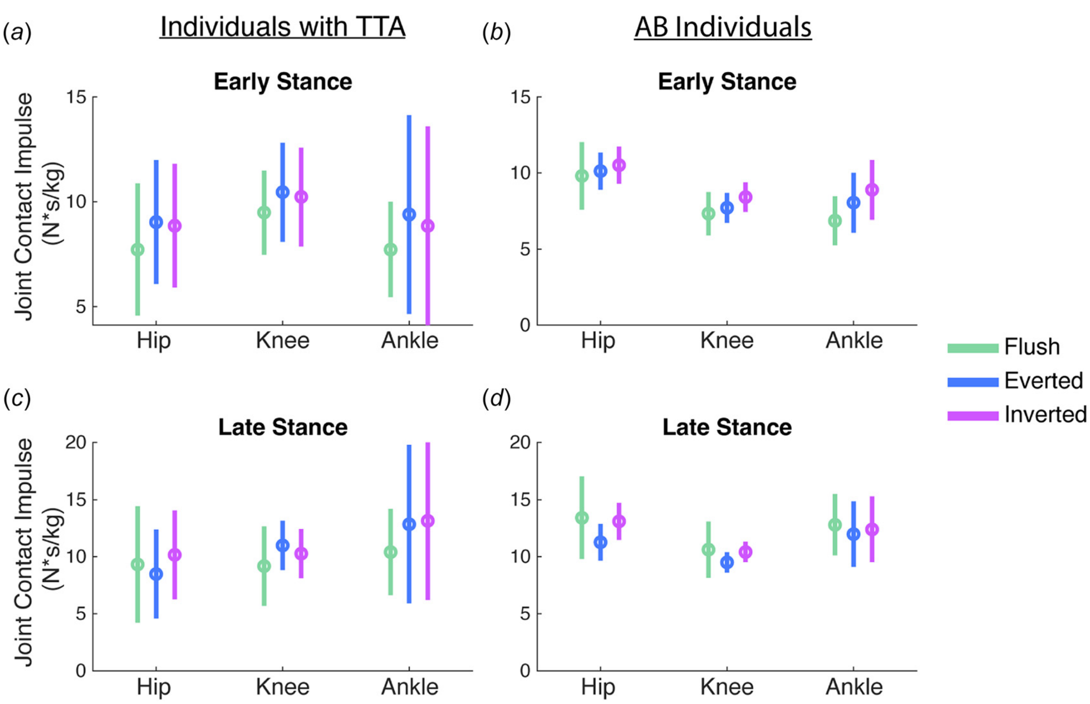

Fig. 4 **(*a*) Intact limb for individuals with TTA and (*b*) nondominant limb for AB individuals joint contact impulse (JCI) during early stance in the flush, everted, and inverted uneven step conditions. (*c*) Intact limb for individuals with TTA and (*d*) nondominant limb for AB individuals JCI during late stance in the flush, everted and inverted uneven step conditions. Early and late stance are determined by the first or second half of stance, respectively. All impulses are normalized by body mass. Open circles represent mean JCI and vertical bars represent 95% confidence intervals for each condition.**

forces contribute to joint loading [34,35]. Although magnitudes presented in this study are higher than in vivo measurements, which show knee contact forces around three times larger than bodyweight for AB individuals [24], these results are comparable to those reported in previous simulation studies for individuals with TTA walking on level ground [17]. Additionally, simulated hip contact forces are estimated between 4 and 6 times bodyweight [47,48], so these results fall within this range. Further, individuals with TTA and AB individuals were simulated with the same framework, so comparing relative changes between groups would not change based on methods of measuring joint loading. The threshold of 10% selected as a notable change was selected based on a minimum-detectable change computed in knee joint loading for healthy individuals. While this measure was extrapolated to individuals with TTA and other joints, the 10% difference between conditions was found to be a conservative measure compared to the values in Barrios and Willson [41].

A potential model limitation is the prosthetic socket and residual limb interface was assumed to be rigid. Previous work has shown that additional socket degrees-of-freedom reduce kinematic error [39]. However, our simulations tracked experimental data very closely. This study only examined axial joint contact forces, so future work should investigate how additional degrees-of-freedom impact joint contact forces in other planes.

Further, the simulation results were highly variable (Figs. 2 and 4), which may be due to individual subjects using different recovery strategies in response to the uneven surface. Individuals with TTA completed the protocol with their clinically prescribed prosthesis, which was not standardized across participants and could have also contributed to the variability of the results. However, the clinically prescribed prosthesis includes components thought by both the clinician and the patient to be optimal for their daily activities and required no acclimation period. Since the simulations relied on experimental data where only five individuals with TTA were able to complete all conditions, it is difficult to generalize the results due to the different strategies used. While the results may be difficult to generalize, the trends observed in JCF and JCI between conditions suggest there may be increased risk for joint pain or injury for those with lower-limb amputations. Future work should increase the sample size to improve the generalizability of the results and identify minimal clinically important differences.

5 Conclusion

This simulation study highlights that individuals with TTA walking over uneven terrain experience altered joint loading patterns in comparison to level-ground walking, with increased residual limb JCF and JCI during the uneven step and increased intact limb JCF and JCI during the recovery step for the knee and ankle joints. The relative increases between the uneven surface and flush conditions in knee JCF and JCI during the uneven and recovery steps were larger than in AB individuals. High variability in these results demonstrates different responses to uneven surfaces when an ankle-foot prosthesis has limited degrees-of-freedom. Future work should investigate whether a prosthesis with an adapting ankle can mitigate these altered loads to reduce joint pain and injury risk, which would provide clinicians the ability to prescribe adapting ankle prostheses for individuals with TTA who often ambulate outdoors and encounter uneven terrain.

Funding Data

- US Department of Veterans Affairs (Grant No. I50 RX002357, IK6 RX002974, and I01 RX001840; Funder ID: 10.13039/100000738).

Data Availability Statement

The datasets generated and supporting the findings of this article are obtainable from the corresponding author upon reasonable request.

Appendix A

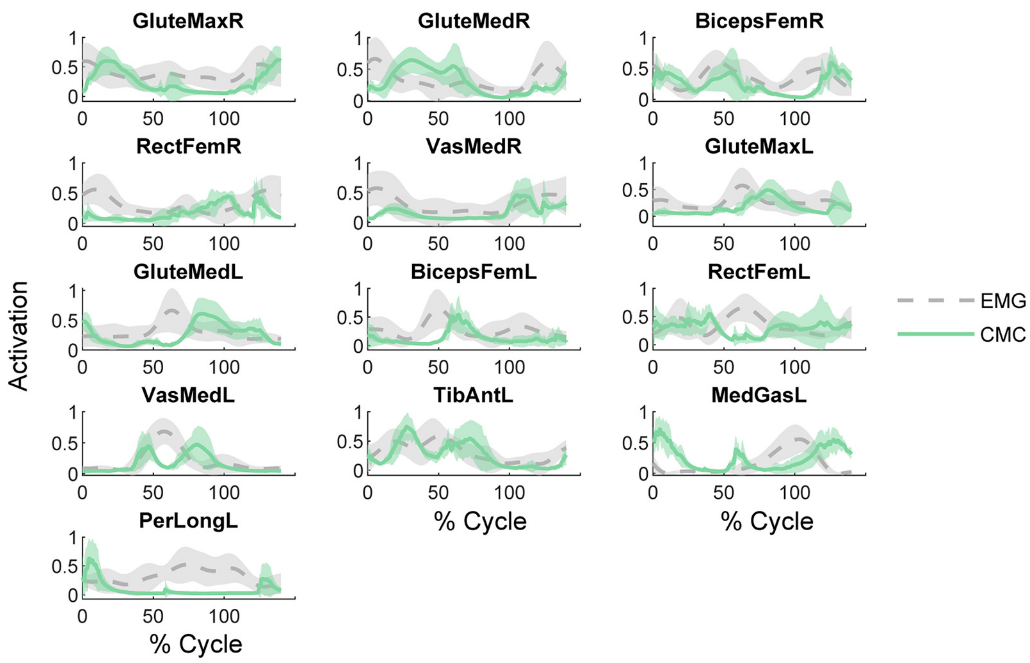

Fig. 5 Normalized muscle activation results for individuals with TTA walking on a flush surface comparing electromyography (EMG) data (dashed line) to simulation results (solid line). Shaded region represents ±1 standard deviation. EMG is shown for both steps throughout the trial, time normalized to the residual limb gait cycle.

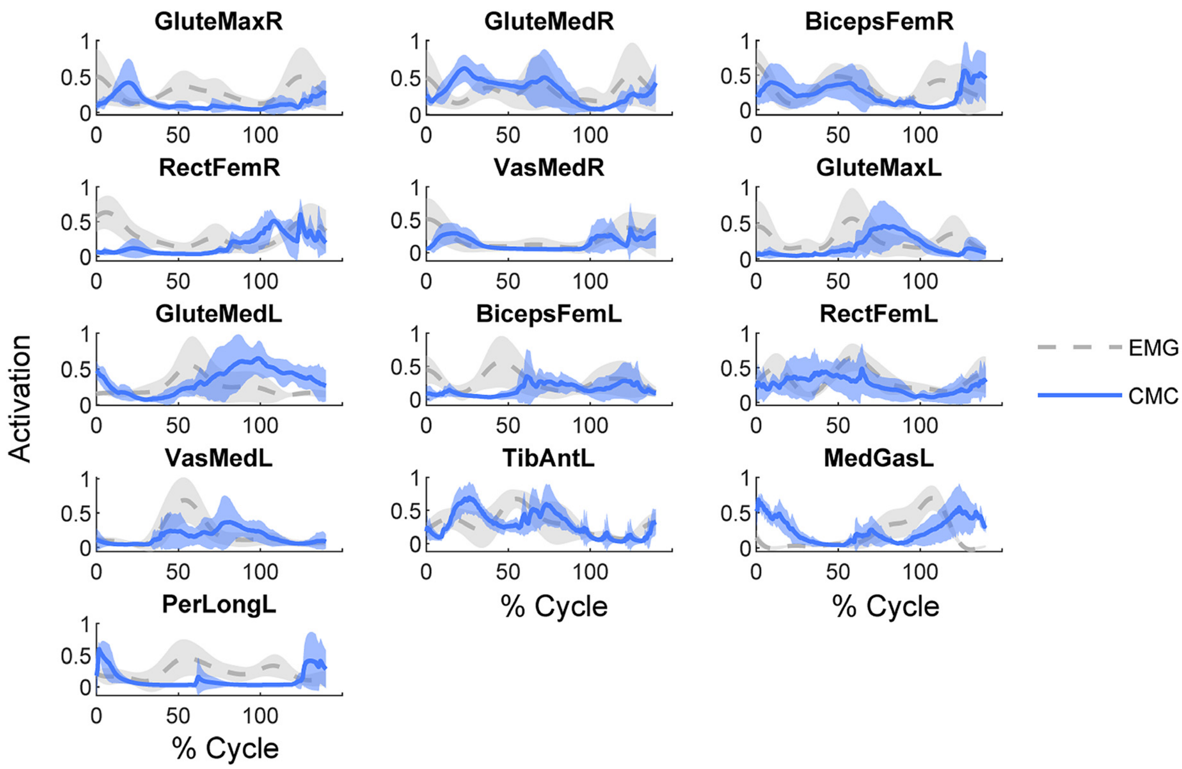

Fig. 6 **Normalized muscle activation results for individuals with TTA walking on an everted surface comparing electromyography (EMG) data (dashed line) to simulation results (solid line). Shaded region represents ±1 standard deviation. EMG is shown for both steps throughout the trial, time normalized to the residual limb gait cycle.**

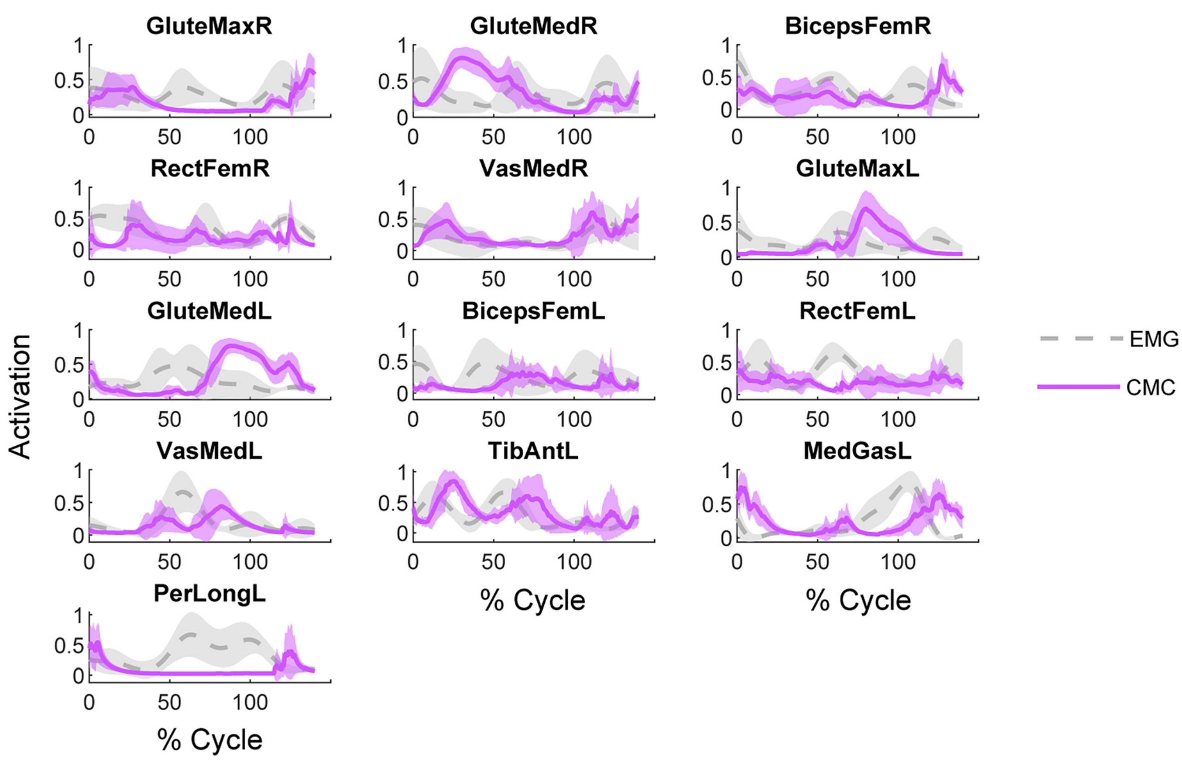

Fig. 7 **Normalized muscle activation results for individuals with TTA walking on an inverted surface comparing electromyography (EMG) data (dashed line) to simulation results (solid line). Shaded region represents ±1 standard deviation. EMG is shown for both steps throughout the trial, time normalized to the residual limb gait cycle.**

Appendix B

Table 1 Mean ±1 Standard Deviation percent differences in peak joint contact forces (JCF) between uneven surface conditions (i.e., everted and inverted) and flush for individuals with TTA

		Uneven step		Recovery step	
Variable	Condition	Early stance	Late stance	Early stance	Late stance
Peak hip JCF (% increase from flush)	Everted	**10.52** ± **5.78**	**−14.02** ± **13.73**	**23.83** ± **11.14**	**−19.33** ± **8.46**
	Inverted	−8.41 ± 3.78	−8.56 ± 7.07	**14.28** ± **6.04**	**12.75** ± **4.26**
Peak knee JCF (% increase from flush)	Everted	**29.88** ± **14.72**	4.82 ± 2.04	**10.92** ± **3.19**	**17.65** ± **3.90**
	Inverted	8.95 ± 4.60	4.61 ± 2.00	**16.16** ± **5.42**	**26.39** ± **5.74**
Peak ankle JCF (% increase from flush)	Everted	9.52 ± 1.56	−4.32 ± 3.77	**15.42** ± **6.21**	**19.54** ± **7.84**
	Inverted	2.84 ± 0.44	−1.53 ± 0.29	**10.81** ± **2.58**	**39.24** ± **17.72**

Percent differences larger than 10 percent are bolded and underlined.

Table 2 Mean ±1 standard deviation percent differences in peak joint contact forces (JCF) between uneven surface conditions (i.e., everted and inverted) and flush for AB individuals

		Uneven step		Recovery step	
Variable	Condition	Early stance	Late stance	Early stance	Late stance
Peak hip JCF (% increase from flush)	Everted	**17.89** ± **5.40**	2.31 ± 1.39	5.42 ± 3.05	**−10.08** ± **7.72**
	Inverted	**12.19** ± **2.99**	**−16.49** ± **8.89**	5.89 ± 3.65	5.59 ± 4.33
Peak knee JCF (% increase from flush)	Everted	**14.12** ± **5.22**	−7.80 ± 4.88	**40.41** ± **17.89**	−9.78 ± 7.50
	Inverted	**13.75** ± **5.15**	**−19.95** ± **12.76**	**41.25** ± **14.38**	2.45 ± 1.90
Peak ankle JCF (% increase from flush)	Everted	**35.40** ± **24.78**	2.23 ± 1.96	**27.04** ± **9.32**	−2.44 ± 1.90
	Inverted	**24.13** ± **16.66**	**11.70** ± **9.96**	**37.70** ± **15.45**	3.71 ± 2.77

Percent differences larger than 10 percent are bolded and underlined.

Table 3 Mean ± 1 standard deviation percent differences in joint contact impulses (JCI) between uneven surface conditions (i.e., everted and inverted) and flush for individuals with TTA

		Uneven step		Recovery step	
Variable	Condition	Early stance	Late stance	Early stance	Late stance
Hip JCI (% increase from flush)	Everted	−0.08 ± 0.03	**−13.16** ± **9.70**	**16.92** ± **8.10**	−9.06 ± 3.51
	Inverted	−3.51 ± 1.19	**−11.04** ± **7.88**	**14.69** ± **6.97**	9.01 ± 1.38
Knee JCI (% increase from flush)	Everted	**20.26** ± **8.03**	−2.25 ± 0.77	**10.25** ± **2.58**	**19.81** ± **4.53**
	Inverted	**12.08** ± **5.39**	−0.65 ± 0.22	7.87 ± 5.10	**11.92** ± **2.59**
Ankle JCI (% increase from flush)	Everted	**16.67** ± **5.18**	−8.91 ± 2.47	**21.57** ± **8.53**	**23.45** ± **7.97**
	Inverted	5.81 ± 0.83	2.79 ± 0.56	**14.64** ± **3.42**	**26.37** ± **8.78**

Percent differences larger than 10 percent are bolded and underlined.

Table 4 Mean ± 1 standard deviation percent differences in joint contact impulses (JCI) between uneven surface conditions (i.e., everted and inverted) and flush for AB individuals.

		Uneven step		Recovery step	
Variable	Condition	Early stance	Late stance	Early stance	Late stance
Hip JCI (% increase from flush)	Everted	−0.75 ± 0.23	−8.94 ± 5.35	3.19 ± 1.40	**−16.02** ± **12.80**
	Inverted	4.03 ± 11.83	**−14.47** ± **10.34**	7.19 ± 3.35	−2.34 ± 3.60
Knee JCI (% increase from flush)	Everted	4.53 ± 1.80	−8.25 ± 2.81	5.18 ± 1.92	**−10.55** ± **7.65**
	Inverted	4.19 ± 1.87	**−16.07** ± **0.22**	**14.76** ± **9.61**	−1.96 ± 1.39
Ankle JCI (% increase from flush)	Everted	**57.69** ± **5.18**	−1.40 ± 2.47	**17.28** ± **6.02**	−6.38 ± 4.01
	Inverted	**35.55** ± **0.83**	−2.60 ± 0.56	**29.58** ± **10.43**	−3.15 ± 1.86

Percent differences larger than 10 percent are bolded and underlined.

References

[1] Li, W., Keegan, T. H. M., Sternfeld, B., Sidney, S., Quesenberry, C. P., and Kelsey, J. L., 2006, "Outdoor Falls Among Middle-Aged and Older Adults: A Neglected Public Health Problem," Am. J. Public Health, **96**(7), pp. 1192–1200.

[2] Steinberg, N., Gottlieb, A., Siev-Ner, I., and Plotnik, M., 2019, "Fall Incidence and Associated Risk Factors Among People With a Lower Limb Amputation During Various Stages of Recovery–a Systematic Review," Disabil. Rehabil., **41**(15), pp. 1778–1787.

[3] Segal, A. D., Yeates, K. H., Neptune, R. R., and Klute, G. K., 2018, "Foot and Ankle Joint Biomechanical Adaptations to an Unpredictable Coronally Uneven Surface," ASME J. Biomech. Eng., **140**(3), p. 031004.

[4] MacKinnon, C. D., and Winter, D. A., 1993, "Control of Whole Body Balance in the Frontal Plane During Human Walking," J. Biomech., **26**(6), pp. 633–644.

[5] Hof, A. L., van Bockel, R. M., Schoppen, T., and Postema, K., 2007, "Control of Lateral Balance in Walking. Experimental Findings in Normal Subjects and Above-Knee Amputees," Gait Posture, **25**(2), pp. 250–258.

[6] Brough, L. G., Klute, G. K., and Neptune, R. R., 2021, "Biomechanical Response to Mediolateral Foot-Placement Perturbations During Walking," J. Biomech., **116**, p. 110213.

[7] Yeates, K. H., Segal, A. D., Neptune, R. R., and Klute, G. K., 2016, "Balance and Recovery on Coronally-Uneven and Unpredictable Terrain," J. Biomech., **49**(13), pp. 2734–2740.

[8] Miller, S. E., Segal, A. D., Klute, G. K., and Neptune, R. R., 2018, "Hip Recovery Strategy Used by Below-Knee Amputees Following Mediolateral Foot Perturbations," J. Biomech., **76**, pp. 61–67.

[9] Cyr, K. M., Segal, A. D., Neptune, R. R., and Klute, G. K., 2023, "Biomechanical Responses of Individuals With Transtibial Amputation Stepping on a Coronally Uneven and Unpredictable Surface," J. Biomech., **155**, p. 111622.

[10] Silverman, A. K., and Neptune, R. R., 2011, "Differences in Whole-Body Angular Momentum Between Below-Knee Amputees and Non-Amputees Across Walking Speeds," J. Biomech., **44**(3), pp. 379–385.

[11] Sheehan, R. C., Beltran, E. J., Dingwell, J. B., and Wilken, J. M., 2015, "Mediolateral Angular Momentum Changes in Persons With Amputation During Perturbed Walking," Gait Posture, **41**(3), pp. 795–800.

[12] Neptune, R. R., and Vistamehr, A., 2019, "Dynamic Balance During Human Movement: Measurement and Control Mechanisms," ASME J. Biomech. Eng., **141**(7), p. 070801.

[13] Yeates, K. H., Segal, A. D., Neptune, R. R., and Klute, G. K., 2018, "A Coronally Clutching Ankle to Improve Amputee Balance on Coronally Uneven and Unpredictable Terrain," ASME J. Med. Devices, **12**(3), p. 031001.

[14] Gates, D. H., Dingwell, J. B., Scott, S. J., Sinitski, E. H., and Wilken, J. M., 2012, "Gait Characteristics of Individuals With Transtibial Amputations Walking on a Destabilizing Rock Surface," Gait Posture, **36**(1), pp. 33–39.

[15] Koelewijn, A. D., and van den Bogert, A. J., 2016, "Joint Contact Forces Can Be Reduced by Improving Joint Moment Symmetry in Below-Knee Amputee Gait Simulations," Gait Posture, **49**, pp. 219–225.

[16] Miller, R. H., Krupenevich, R. L., Pruziner, A. L., Wolf, E. J., and Schnall, B. L., 2017, "Medial Knee Joint Contact Force in the Intact Limb During Walking in Recently Ambulatory Service Members With Unilateral Limb Loss: A Cross-Sectional Study," PeerJ, **5**(2), p. e2960.

[17] Silverman, A. K., and Neptune, R. R., 2014, "Three-Dimensional Knee Joint Contact Forces During Walking in Unilateral Transtibial Amputees," J. Biomech., **47**(11), pp. 2556–2562.

[18] Maly, M. R., 2009, "Linking Biomechanics to Mobility and Disability in People With Knee Osteoarthritis," Exerc. Sport Sci. Rev., **37**(1), pp. 36–42.

[19] Foroughi, N., Smith, R., and Vanwanseele, B., 2009, "The Association of External Knee Adduction Moment With Biomechanical Variables in Osteoarthritis: A Systematic Review," Knee, **16**(5), pp. 303–309.

[20] Burke, M. J., Roman, V., and Wright, V., 1978, "Bone and Joint Changes in Lower Limb Amputees," Ann. Rheum. Dis., **37**(3), pp. 252–254.

[21] Norvell, D. C., Czerniecki, J. M., Reiber, G. E., Maynard, C., Pecoraro, J. A., and Weiss, N. S., 2005, "The Prevalence of Knee Pain and Symptomatic Knee Osteoarthritis Among Veteran Traumatic Amputees and Nonamputees," Arch. Phys. Med. Rehabil., **86**(3), pp. 487–493.

[22] Struyf, P. A., van Heugten, C. M., Hitters, M. W., and Smeets, R. J., 2009, "The Prevalence of Osteoarthritis of the Intact Hip and Knee Among Traumatic Leg Amputees," Arch. Phys. Med. Rehabil., **90**(3), pp. 440–446.

[23] Morgenroth, D. C., Gellhorn, A. C., and Suri, P., 2012, "Osteoarthritis in the Disabled Population: A Mechanical Perspective," PM R, **4**(5S), pp. S20–S27.

[24] Kutzner, I., Heinlein, B., Graichen, F., Bender, A., Rohlmann, A., Halder, A., Beier, A., and Bergmann, G., 2010, "Loading of the Knee Joint During Activities of Daily Living Measured In Vivo in Five Subjects," J. Biomech., **43**(11), pp. 2164–2173.

[25] D'Lima, D. D., Patil, S., Steklov, N., Slamin, J. E., and Colwell, C. W., Jr, 2005, "In Vivo Knee Forces After Total Knee Arthroplasty," Clin. Orthop. Relat. Res., **440**(&NA), pp. 45–49.

[26] Taylor, S. J. G., Walker, R. S., Perry, J. S., Cannon, S. R., and Woledge, R., 1998, "The Forces in the Distal Femur and the Knee During Walking and Other Activities Measured by Telemetry," J. Arthroplasty, **13**(4), pp. 428–437.

[27] Mündermann, A., Dyrby, C. O., D'Lima, D. D., Colwell, C. W., Jr., and Andriacchi, T. P., 2008, "In Vivo Knee Loading Characteristics During Activities of Daily Living as Measured by an Instrumented Total Knee Replacement," J. Orthop. Res., **26**(9), pp. 1167–1172.

[28] Pruziner, A. L., Werner, K. M., Copple, T. J., Hendershot, B. D., and Wolf, E. J., 2014, "Does Intact Limb Loading Differ in Servicemembers With Traumatic Lower Limb Loss?," Clin. Orthop. Relat. Res., **472**(10), pp. 3068–3075.

[29] Fey, N. P., and Neptune, R. R., 2012, "3D Intersegmental Knee Loading in Below-Knee Amputees Across Steady-State Walking Speeds," Clin. Biomech., **27**(4), pp. 409–414.

[30] Doyle, S. S., Lemaire, E. D., Nantel, J., and Sinitski, E. H., 2019, "The Effect of Surface Inclination and Limb on Knee Loading Measures in Transtibial Prosthesis Users," J. Neuroeng. Rehabil., **16**(1), pp. 1–8.

[31] Miyazaki, T., Wada, M., Kawahara, H., and Sato, M., 2002, "Dynamic Load at Baseline Can Predict Radiographic Disease Progression in Medial Compartment Knee Osteoarthritis," Ann. Rheum. Dis., **61**(7), pp. 617–622.

[32] Kutzner, I., Trepczynski, A., Heller, M. O., and Bergmann, G., 2013, "Knee Adduction Moment and Medial Contact Force-Facts About Their Correlation During Gait," PLoS One, **8**(12), p. e81036.

[33] Walter, J. P., D'Lima, D. D., Colwell, C. W., Jr,., and Fregly, B. J., 2010, "Decreased Knee Adduction Moment Does Not Guarantee Decreased Medial Contact Force During Gait," J. Orthop. Res., **28**(10), pp. 1348–1354.

[34] Shelburne, K. B., Torry, M. R., and Pandy, M. G., 2006, "Contributions of Muscles, Ligaments, and the Ground-Reaction Force to Tibiofemoral Joint Loading During Normal Gait," J. Orthop. Res., **24**(10), pp. 1983–1990.

[35] Sasaki, K., and Neptune, R. R., 2010, "Individual Muscle Contributions to the Axial Knee Joint Contact Force During Normal Walking," J. Biomech., **43**(14), pp. 2780–2784.

[36] Stewart, K. M., Klute, G., and Neptune, R. R., 2023, "Simulated Able-Bodied Lower-Limb Joint Loading While Walking on Unexpected Uneven Terrain," *TechRxiv*.

[37] Sangeux, M., and Polak, J., 2015, "A Simple Method to Choose the Most Representative Stride and Detect Outliers," Gait Posture, **41**(2), pp. 726–730.

[38] Delp, S. L., Anderson, F. C., Arnold, A. S., Loan, P., Habib, A., John, C. T., Guendelman, E., and Thelen, D. G., 2007, "OpenSim: Open-Source Software to Create and Analyze Dynamic Simulations of Movement," IEEE Trans. Biomed. Eng., **54**(11), pp. 1940–1950.

[39] LaPrè, A. K., Price, M. A., Wedge, R. D., Umberger, B. R., and Sup, F. C., 2018, "Approach for Gait Analysis in Persons With Limb Loss Including Residuum and Prosthesis Socket Dynamics," Int. J. Numer. Method Biomed. Eng., **34**(4), p. e2936.

[40] Thelen, D. G., and Anderson, F. C., 2006, "Using Computed Muscle Control to Generate Forward Dynamic Simulations of Human Walking From Experimental Data," J. Biomech., **39**(6), pp. 1107–1115.

[41] Barrios, J., and Willson, J., 2017, "Minimum Detectable Change in Medial Tibiofemoral Contact Force Parameters: Derivation and Application to a Load-Altering Intervention," J. Appl. Biomech., **33**(2), pp. 171–175.

[42] Paysant, J., Beyaert, C., Dati, A.-M., Martinet, N., and Andr, J.-M., 2006, "Influence of Terrain on Metabolic and Temporal Gait Characteristics of Unilateral Transtibial Amputees," J. Rehabil. Res. Dev., **43**(2), pp. 153–160.

[43] Kent, J. A., Takahashi, K. Z., and Stergiou, N., 2019, "Uneven Terrain Exacerbates the Deficits of a Passive Prosthesis in the Regulation of Whole Body Angular Momentum in Individuals With a Unilateral Transtibial Amputation," J. Neuroeng. Rehabil., **16**(1), pp. 1–10.

[44] Moisan, G., Miramand, L., Younesian, H., Legrand, T., and Turcot, K., 2021, "Assessment of Biomechanical Deficits in Individuals With a Trans-Tibial Amputation During Level Gait Using One-Dimensional Statistical Parametric Mapping," Gait Posture, **87**, pp. 130–135.

[45] Nolan, L., and Lees, A., 2000, "The Functional Demands on the Intact Limb During Walking for Active Trans-Femoral and Trans-Tibial Amputees," Prosthet. Orthot. Int., **24**(2), pp. 117–125.

[46] Roelker, S. A., Caruthers, E. J., Hall, R. K., Pelz, N. C., Chaudhari, A. M. W., and Siston, R. A., 2020, "Effects of Optimization Technique on Simulated Activations and Forces," J. Appl. Biomech., **36**(4), pp. 259–278.

[47] Correa, T. A., Crossley, K. M., Kim, H. J., and Pandy, M. G., 2010, "Contributions of Individual Muscles to Hip Joint Contact Force in Normal Walking," J. Biomech., **43**(8), pp. 1618–1622.

[48] Giarmatzis, G., Jonkers, I., Wesseling, M., Van Rossom, S., and Verschueren, S., 2015, "Loading of Hip Measured by Hip Contact Forces at Different Speeds of Walking and Running," JBMR, **30**(8), pp. 1431–1440.